Study of structural, elastic & thermal properties of DyMg alloy using the FP-LAPW method

Meena Kumari*, Manju Sikarwar, U.P.Verma**

School of Studies in Physics, Jiwaji University, Gwalior 474 011, India

**Corresponding authors; Tel: (0751) 2772782; E-mail: meenaranot@gmail.com, upv.udai@gmail.com

Received: 31 March 2016, Revised: 30 September 2016 and Accepted: 16 June 2017

DOI: 10.5185/amp.2017/726
www.vbripress.com/amp

Abstract

In this paper DyMg alloy has been studied in three phases viz. B1, B2 and B3. The exchange correlation potential within the generalized-gradient approximation (GGA) of projector augmented wave (PAW) method is used. The predicted lattice constants and total energy at ambient condition, respectively in B1, B2 and B3 phases are 6.395, 3.772, 6.40 Å, and -24734.778, -24734.855, -24734.683 Ry. From the calculations it is evident that ground state phase of DyMg is B2, therefore, other parameters such as the bulk modulus, its pressure derivative, elastic constants and thermal properties related to B2 phase are presented in this paper. The obtained results are compared with the available experimented and theoretical data. The calculated band structure shows that this alloy no band gap. In order to obtain more information about the elastic properties other parameters such as Zener anisotropy factor, Poisson ratio, Young's modulus and isotropic shear modulus are also presented. Thermal parameter such as Debye temperature, specific heat, Gruneisen parameter etc. has been determined as a function of pressure and temperature. Copyright © 2017 VBRI Press.

Keywords: DFT, band structure, elastic property, magnesium alloy, thermal properties.

Introduction

Magnesium and magnesium alloy possess many unique properties. These are the high specific strength, low density, Young's modulus and good stiffness. They also show high degree of biocompatibility [**1-5**]. Prominent technological importance of magnesium alloys is in the automobile and aircraft industry [**6**]. For magnesium alloys the rare earth elements are promising alloying elements which have many interesting biomedical applications [**7**]. In fact, alloy formed due to the addition of Rare Earth (RE) Elements into Mg have significant effects on its creep resistance as well as the high temperature strength [**8**]. It also improves remarkably the magnesium corrosion resistance [**7, 9**]. Electronic configuration of the atom Magnesium is $1s^2$, $2s^2$, $2p^6$, $3s^2$ which has no *d*-electron and has a larger atomic radius; therefore, a different magnetic behavior has been expected for REMg. Aleonard et al. [**10**] have performed neutron powder diffraction measurement for understanding the magnetic properties of the rare earth magnesium compounds. Belakhovsky et al. [**11**] have also studied the magnetic properties of DyMg and ErMg using Mössbauer spectroscopy. In an early work, Buschow et al. [**12**] have analyzed the crystal structures and some physical properties of the intermetallics compounds of the rare earth (from La to Lu) and non-magnetic metals (B, Be, Mg, Ru, Rh, Pd) experimentally. Buschow et al [**13**] and Kirchmayr at el. [**14**] have reported the magnetic properties of REMg compounds. Zhang et al. [**15**] have predicted the enthalpy of formation of MgX(X = As, Ba, Ca, Cd, Cu, Dy, Ga, Ge, La, Ni, Lu, Pb, Si, Sn and Y) compounds from the first-principles calculations. The Brittle and elastic properties of the MgRE (RE = Sc, Y, Pr, Nd, Dy, Ho, Er) have been determined by Wu and Hu [**16**] using the density functional calculations. Villars et al [**17**] have presented the intermetallics phases in their hand book of crystallographic data. The elastic properties of REMg (RE = Sc, Y, La–Lu) intermetallics compounds have been calculated at T = 0K by Tao et al. [**18**] employing the generalized gradient approximation (GGA). Wang et al. [**19**] have studied lattice dynamical and thermodynamic properties such as thermal expansion, bulk modulus, heat capacities at constant volume and constant pressure as a function of temperature of the rare earth magnesium intermetallics compounds MgRE (RE=Y, Dy, Pr, Tb) using density functional theory and density functional perturbation theory. They have also computed the temperature-dependent elastic properties and second and third order elastic constants for same family in CsCl type structure.

The thermodynamic properties and elastic constants of Mg-Pr, Mg-Dy and Mg-Y intermetallics as a function of temperature are also estimated by Wu et al. [**20, 22**]. Tao et al. [**23**] focused on phase stability and electronic properties of Mg-RE (RE=Sc, Y) from first principle calculation. Luca et al. [**24**] have reported that the compounds in the rare-earth magnesium series show an unusual behavior (reluctance to oxidize) among rare earth intermetallic that reduce the contribution of the oxidized surface to the scattering phenomena and favors the

observation of multipolar reflections. From the literature survey it is clear that the thermal properties of the rare-earth magnesium alloy are lacking. Therefore, it's worthwhile to study the structural, electronic, elastic and thermal properties of DyMg.

In this paper we report the first principal calculation within the frame of density functional theory (DFT) using the full potential linearized augmented plane wave (FP-LAPW) method to study the structural, electronic, elastic and thermal properties of DyMg in CsCl (B2) type structure. The predictions of these physical properties of DyMg may play a vital role to the design of heat-resistant magnesium alloys.

Computational details

All calculations in the present study are based on the implementation of plane wave density functional theory (DFT), according to which the many body problem of interacting electrons and nuclei is mapped to a series of one electron equations called the Khon-Sham equations. We used the self consistent full linearized augmented plane wave (FP-LAPW) method to solve the Khon –Sham equations as implemented in the WIEN-2k code [**25**]. The exchange and correlation effects were treated by using the form of GGA proposed by Wu and Cohen (WC-GGA) [**26**]. The valance electronic configurations are $3s^2$ for Mg *and* $6s^2\ 4f^{10}$ for Dy. To achieve the energy Eigen values convergence, the calculations were performed with $R_{MT}k_{max}= 7$, where R_{MT} is the smallest radii of the muffin-tin spheres and k_{max} is the maximum modulus for the reciprocal lattice vector. The values of muffin-tin radii (R_{MT}) for Dy and Mg were taken as 3.0 and 2.2 Bohr, respectively. The maximum value for the angular momentum quantum *l*=10 is adopted for the wave function expansion inside the atomic sphere. The dependency of the total energy on the number of k-points in the irreducible wedge of Brillouin zone has been optimized and the size of mesh has been set to $10 \times 10 \times 10$ k-points for B2 structure of DyMg. Self consistency is considered to be reached when total energy difference between successive iterations is less than 10^{-5} Ryd per formula unit and charge converges to less than $0.001e^-$.The temperature effects for DyMg have been determined by using quasiharmonic Debye model as implemented in GIBBS code [**27**]. This model generates Debye temperature Θ_D (V) and obtains the non-equilibrium Gibbs function G*(V; P, T) and minimize G* to derive the thermal equation of state V (P, T). In the quasi-harmonic Debye model the non-equilibrium Gibbs functions G*(V; P, T) is written as:

$$G^*(V;P,T) = E(V) + PV + A_{vib}(\Theta(V);T)$$

where E (V) is the total energy per unit cell, PV is the product of hydrostatic pressure and unit cell volume that corresponds to the constant hydrostatic pressure condition and A_{vib} is the Helmholtz free energy.

For an isotopic solid the Debye temperature, θ_D is expressed as

$$\Theta_D = \frac{\hbar}{k}\left[6\pi^2 V^{1/2} n\right]^{1/3} f(\sigma)\sqrt{\frac{B_S}{M}}$$

where M is the molecular mass per formula unit and B_S is the adiabatic bulk modulus. Details on $f(\sigma)$ can be found in Refs. [**28, 29**]. Further, B_S is approximated by the static compressibility as

$$B_S \cong B(V) = V\frac{d^2E(V)}{dv^2}$$

Now the thermal equation of state V (P,T) can be obtained minimizing the non equilibrium Gibbs function G* (V; P, T) with respect to volume V given as

$$\left(\frac{\partial G^*(V;P,T)}{\partial V}\right)_{P,T} = 0$$

Thus with the help of the Quasi harmonic Debye model, the thermal quantities at any temperature and pressure of DyMg may be calculated using various sets of the E-V data at ambient condition. The standard thermodynamic relations are used to derive other macroscopic properties of DyMg.

Results and discussion

Structural parameters

For understanding the properties of solids study of the structural properties are very important. In order to obtain ground state structure at ambient condition we studied DyMg in three different phases, viz. B1, B2, and B3. The structure of phase B1 is NaCl type whose space group is known as *Fm3m* and identified by the number 225. The structure of phase B2 is CsCl type whose space group is known as *Pm-3m* and identified by the number 216. The Zincblende structure in known as phase B3 identified by space group F43m and number 216). In B1 and B2 phases atom Dy was placed at (0, 0, 0) position and atom Mg at (0.5, 0.5, 0.5) position while in B3 phase atom Dy was placed at (0, 0, 0) position and atom Mg at (0.25, 0.25, 0.25) position. Using the first-principles approach first we obtained converged total energy corresponding to different unit cell volume. The obtained sets of energy-volume data were fitted to the Murnaghan equation of state [**30**]. The equilibrium structural parameters present obtained are shown in **Table 1** along with experimental and earlier reported available results. This table shows that the structural parameters calculated using GGA functional are in good agreement with earlier reported results [**31**]. **Table 1** also reveals the fact that at ambient condition ground state of DyMg alloy is B2 phase.

Table 1. Comparison of the calculated lattice constant, a(Å), the bulk modulus B_0 (GPa), bulk modulus first pressure derivative B_0' and total energy E_0 (Ry) of DyMg along with the available theoretical and experimental data in B1, B2 and B3 phases.

Material	Phase		a (Å)	B_0	B_0'	E_0
DyMg	B1	P.W	6.395	18.89	3.64	-24734.77
		Other	6.242	33.79	3.7	-
	B2	P.W	3.77	30.26	5.00	24734.86
		Exp.	3.76[10]	-	-	-
	B3	Other	3.77[31]	40.00	3.36	-
		P.W.	7.28	9.51	3.37	-24734.68
		Other	7.06[31]	14.63	3.58	-

Electronic properties

On the basis of the structural parameters at ambient condition the electronic band structure as well as the electronic density of states of DyMg has been shown in this section. To comprehend the mechanism of alloying effects on electronic behavior of DyMg, above two properties are very helpful. The band structure plot for B2 structure of DyMg has been shown in **Fig. 1**. The symmetry points included in the band structure plot are R, Γ, X, M and Γ and the bands are computed along the high symmetry directions in the first Brillouin zone. In figure valence and conduction bands are overlapped at the Fermi level (EF = 0 eV). This suggests that DyMg indicates metallic behavior.

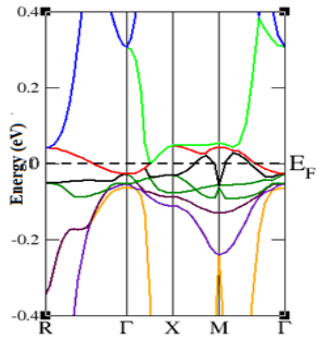

Fig. 1. Calculated Band structure of DyMg in B2 phase.

The total electronic density of state (DOS) and partial density of state (PDOS) plots are shown in **Fig. 2.** The electronic density of state is helpful to the understanding of the bonding characteristics of the studied alloy. The total DOS of DyMg also exhibits non zero values at the Fermi level, which indicates the metallic character of DyMg. **Fig. 2** also indicates that the main contributions in PDOS plot at Fermi level is due to *f* -Dy states.

Elastic properties

Mechanical and dynamical behaviour of crystals are derived from its elastic properties. In fact the forces operating in solids provide important data for developing inter-atomic potentials. The elastic constants are evaluated as per Born's stability criteria which should be satisfied for the stability of lattice [**32**]. The cubic DyMg crystal has three different elastic coefficients (C_{11}, C_{12}, and C_{44}). The known conditions for mechanical stability of cubic crystals are: $C_{11} > 0$, $C_{11} - C_{12} > 0$, $C_{44} > 0$, $C_{11} + 2C_{12} > 0$ and C12 < B < C11. Obtained elastic constants are shown in **Fig. 2**. It is important to note that for DyMg all elastic constants are larger than zero. The Cauchy pressure (C_{12}–C_{44}) can be defined as the angular character of atomic bonding in metals and compounds, which could be related to the brittle/ductile properties of materials [**33, 34**]. In present case obtained Cauchy pressure is -16.70 GPa. Negative Cauchy pressure discrepancy is a consequence of the hybridization of the unstable *f* bands. This hybridization may be responsible for the decrease in Dy-Dy distance and therefore to a small value of the elastic constant C_{12}. The shear modulus G divided by the bulk modulus B denoted as $R_{G/B}$ ratio is roughly a measurement of brittleness or ductility. It is well known that if $R_{G/B} < 0.5$, the material behaves in a ductile manner, and while $R_{G/B} > 0.5$, the material behaves in a brittle manner [**35–37**]. The $R_{G/B}$ value of DyMg alloy in B2 phase has been obtained as 0.56 which indicates that its behavior is brittle. Our present calculated $R_{G/B}$ ratio is in excellent agreement with earlier reported results [**31**].

.

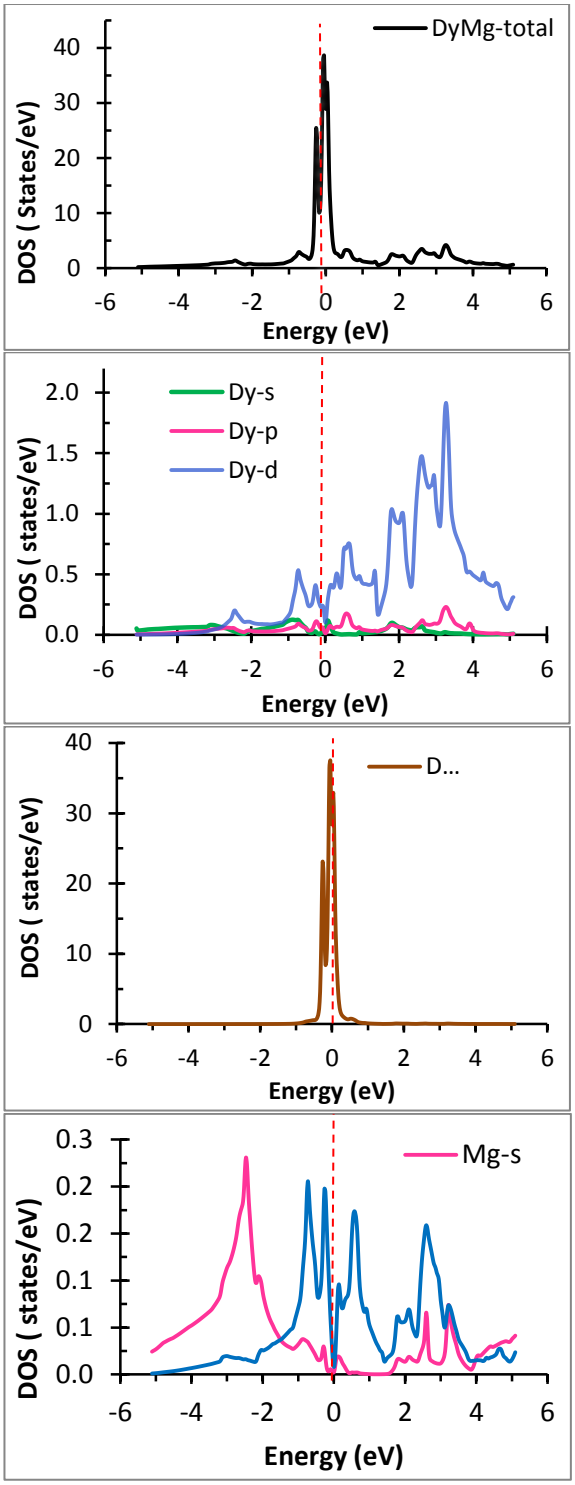

Fig. 2. Total and partial density of states of DyMg in B2 Phase. The Fermi level is set to be 0 eV.

Table 2. Calculated elastic constant (in GPa) with Zener anisotropy factor (A), Poisson ratio (ν), Young's modulus (Y) and isotropic shear modulus (G) in B2 phase of DyMg.

Parameters ↓	PW	Ref. [31]
C_{11}	36.52	52.33
C_{12}	29.18	37.05
C_{44}	45.88	40.37
C_{12}-C_{44}	-16.70	-3.32
A	12.50	5.29
ν	00.26	00.27
Y	46.95	53.79
G	18.60	21.08

Thermal properties

Lattice dynamics is the most important aspects to study the different properties of materials. It deals with the vibrations of the atoms about their mean position. These vibrations are completely responsible for the thermal properties. The thermal properties of DyMg have been determined using quasi harmonic Debye approximation model. In this model the anharmonic effect is accounted for by allowing the phonon frequencies to depend on the crystal volume. The thermal properties are determined in the temperature range 0 - 1000 K. Similarly, pressure effect is studied in the range 0 - 30 GPa. Total energy verses cell volume determined in the previous section has been used to drive the thermal parameters as bulk modulus, thermal expansion, and heat capacity and Gruneisen parameter etc at different temperature and pressures. The calculated results are listed in **Table 3**.

Table 3. Thermal parameter of DyMg in B2 phase at 0K and 300K.

Thermal parameter	DyMg	
	P=0, T=0	P=0, T=300
α	0.00	7.99
B_0 (GPa)	30.92	29.16
Cv (J/mol K)	0.00	48.93
Cp (J/mol K)	0.00	50.79
Debye temp. (K)	192.22	186.60
Gruneisen parameter	1.582	1.585
B_0'	3.48	3.45
Entropy	0.00	90.68

Bulk modulus

A plot of bulk modulus versus pressure for different values of temperature is shown in **Fig 3(a).** The bulk modulus increases with the increase in pressure. Effect of temperature corresponding to pressure is not very significant near lower range of pressure but increases slightly with the increase in pressure.

Thermal expansion coefficient

The thermal expansion coefficient, α, is a function of temperature. It has been analyzed at hydrostatic pressure P = 0, 10, 20 and 30 GPa. Plots of α versus temperature for different values of pressure are shown in **Fig. 3(b).** From **Fig. 3(b),** it is clear that α (T) increases sharply with the increase in temperature up to T = 200 K. Beyond 200 K the rate of increase in α (T) for high pressures becomes slow and approaches a constant value around T = 300 K but corresponding to P= 0 GPa it shows slightly increasing trend. This shows that at a fixed temperature as the pressure increases, its effect on the thermal expansion decreases. Similarly, at a given pressure, P, the effect of increasing temperature on α decreases rapidly.

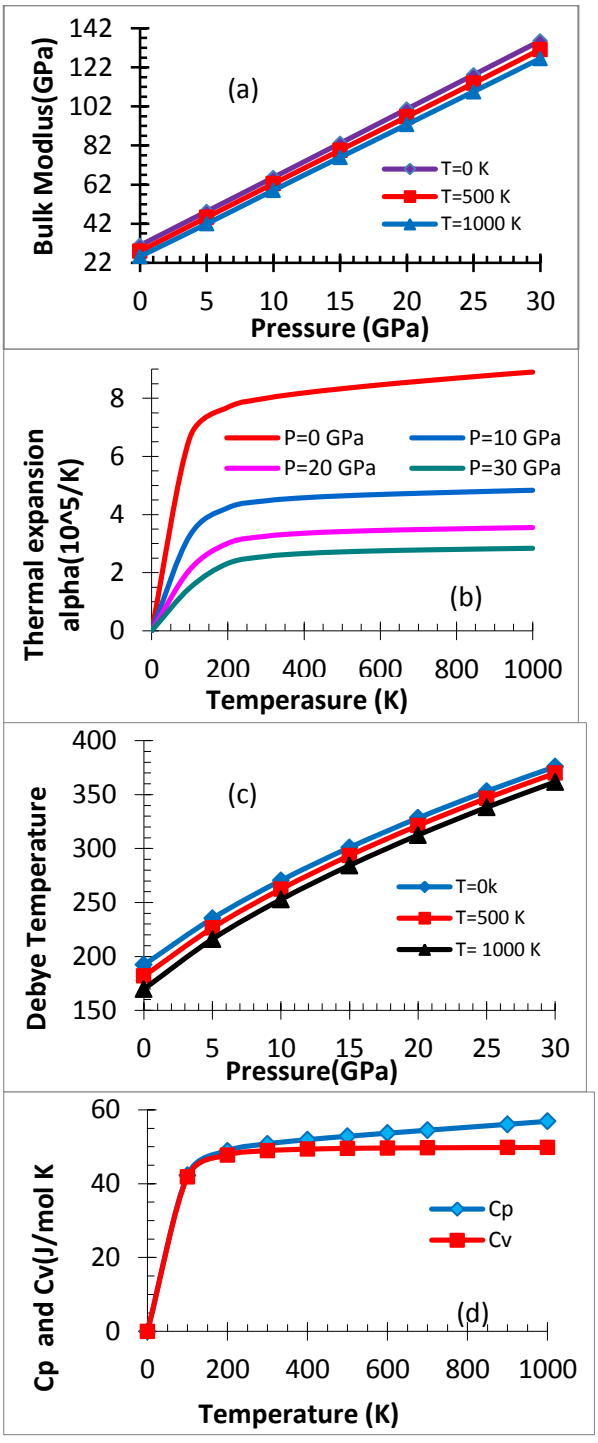

Fig. 3. Thermodynamical parameters of DyMg as functions of temperature T (in K) and pressure (in GPa).

Debye temperature

Fig. 3(c) shows plots of Debye temperature as a function of pressure at different temperatures. In such plots variation is almost linear and the Debye temperature increases with the increase in pressure. Because of inherent relationship of

Debye temperature to the lattice vibrations it is very useful thermal parameter and is basically a measure of the vibrational response of the material. It is, therefore, closely connected with the properties like specific heat, thermal expansion and vibrational entropy.

Specific heat

The specific heat of a material indicates its heat retention or loss ability. Plots of calculated heat capacity of DyMg at constant volume (C_V) and at constant pressure (C_P) as function of temperature are shown in **Fig 3(d)**. The calculated values of C_v and C_P at temperature T= 0K and 300K are given in **Table 3.** From the plots it is observed that at higher temperature C_v tends to a limiting value. The plot of C_P and C_V show that at lower temperature the specific heats are the same but beyond ~110 K, C_P exceeds C_V as a result of thermal expansion of crystal lattice.

Entropy

The entropy is known as the thermodynamic state function of matter and is denoted by symbol S. It describes dispersal of energy and matter. Microscopically this is defined as measure of disorder of the system. As the temperature of the material increases the particles vibrate more vigorously, so the entropy of the system also increases. At high temperature entropy is expressed by the relation

$$S = \text{constant} + NK \ln\left(\frac{T}{\Theta_D}\right)$$

The values of entropy at T=0K and T=300K is given in **Table 3**.

Conclusion

Using the first principal calculation, we have investigated the structural, electronic, elastic and thermal properties of DyMg. The electronic band structure and corresponding DOS plots show metallic nature of alloy. Our calculated structure parameters are in good agreement with the available experimental data. Elastic constants, Zener anisotropy factor, passion ratio's, Young's modulus are also reported. The quasi-harmonic Debye model is successfully applied to determine the thermal properties of in the temperature range 0–1000 K and pressure range 0 – 30 GPa. The thermal parameters such as thermal expansion, Debye temperature, bulk modulus, specific heat, Gruneisen parameter and entropy are also calculated. To the best of our knowledge, there are no previous reports on thermodynamic properties. It is our ambition that these results will spark interest to this compound.

References

1. Waizy, H.; Seitz, J.M.; Reifenrath, J.; Weizbauer, A; Bach, F.W.; Meyer-Lindenberg, A.; Denkena, B.; Windhagen, H.; *J. Mater. Sci.* **2013**, 48, 39–50. **DOI:** 10.1007/s10853-012-6572-2
2. Willbold, E. et al; *Acta Biomater.*, **2013**, 9, 8509–17. **DOI** : 10.1016/j.actbio.2013.02.015
3. Bobe, K. et al.*; Acta Biomater.*, **2013**, 9, 8611–23. **DOI:** 10.1016/j.actbio.2013.03.035
4. Bondarenko, A.; Angrisani, N.; Meyer-Lindenberg, A.; Seitz, JM.; Waizy, H.; Reifenrath, J.; *J. Biomed. Mater. Res., Part A*, **2014**, 102, 1449–57. **DOI**: 10.1002/jbm.a.34828
5. Dziuba, D.; Meyer-Lindenberg, A.; Seitz, JM.; Waizy, H.; Angrisani, N.; Reifenrath; *Acta Biomater.*, **2013**, 9, 8548–60 2013. **DOI:** 10.1016/j.actbio.2012.08.028
6. Mordike, B.L.; Ebert, T.; *Mater. Sci. Eng., A,* **2001**, 302, 37- 45. **DOI:** 10.1016/S0921-5093(00)01351-4
7. Willbold, E. Et al.; *Acta Biomater*., **2015**, 11, 554-562. **DOI**: 10.1016/j.actbio.2014.09.041
8. Kokako, T.; Takadama, H.; *Biomaterials*, **2006**, 27, 2907-15. **DOI**: 10.1016/j.biomaterials.2006.01.017
9. Ding, Y; Wen, C.; Hodgson, P.; Li Y.; *J. Mater. Chem. B.* **2014**, 2, 1912-33. **DOI**: 10.1039/c3tb21746a
10. Aleonard, R.; Morin, P.; Pierre, J.; Schmitt, D.; *J. Phys. F: Met. Phys.*, **1976**, 6. **DOI**: org/0305-4608/9/7/008)
11. Belakhovsky, M.; Chappert, J.; and Schmitt, D.; *J. Phys. C: Solid State Phys.*, **1977,** 10, L493. **DOI:** 10.1088/0022-3719/10/17/006
12. Buschow, K.H. J.; *Rep. Prog. Phys.*, **1979**, 42, 1373. **IOP**: iop.org/0034-4885/42/8/003
13. Buschow, K.H.J.; *J. Less-Common Met.*, **1973**, 33(2) 239-244. **DOI**: 10.1016/0022-5088(73)90043-X
14. Kirchmayr Hans. R., Poldy Carl A., Groessinger R., Haferl R., Hilscher G., Steiner W. , Wiesinger G. , *Handb. Phys. Chem. Rare Earths*, **1979**, 2, 55-230. **DOI**: 10.1016/S0168-1273(79)02005-5
15. Zhang, H.; Shang, S.; Saal J.E.; Saengdeejing, A.; Wang, Y.; Liu, Z.K.; *intermetallics*, **2009**,17, 878-885. **DOI**: 10.1016/j.intermet.2009.03.017
16. Wu, Y.; Hu, W.; *Eur. Phys. J. B*, **2007**, 60, 75-81. **DOI**: 10.1140/epjb/e2007-00323-0
17. P. Villars, L.D. Calvert, Pearson's Handbook of Crystallographic Data for Intermetallic Phases, ASM, Metals Park, OH, 1985. **DOI**: 10.1007/978-3-642-84359-4
18. Tao, X.; Ouyang, Y.; Liu, H.; Feng, Y.; Du, Y.; Jin, Zh.; *Solid State Commun.*, **2008**, 148, 314-318. **DOI**: 10.1016/j.ssc.2008.09.005
19. Wang, R; Wang, S.; Wu, X; *Phys. Scr.*, 2011,83,065707 **DOI**: 10.1088/0031-8949/83/06/065707
20. Wang, R.; Wang, S.; Wu, X.; Yao, Y.; Liu, A.; *Intermetallics*, **2010**, 18, 2472-2476. **DOI**: 10.1016/j.intermet.2010.08.039
21. Wu, Y.; Hu, W.; and Sun, L.; *J. Phys. D: Appl. Phys.*, **2007**, 40, 7584-7592. **DOI**: 10.1088/0022-3727/40/23/052
22. Hu, W.; Xu, H.; Shu., X.; Yuan, X.; Gao, B.; and Zhang, B.; *J. Phys. D: Appl. Phys.*, **2000**, 33, 711-718. **DOI**: 10.1088/0022-3727/33/6/320)
23. Tao, X.; Ouyang, Y.; Liu, H.; Feng, Y.; Du, Y.; He, Y.; Jin, Z.; *J. Alloys Compd.*, **2011**,509, 6899-6907. **DOI**: 10.1016/j.jallcom.2011.03.177
24. Luca, S.E.; Amara, M.; Galera, R.M.; Berar, J.F.; *J. Phys.: Condens. Matter*, **2002**, 14, 935–944. **DOI**: 10.1088/0953-8984/14/4/325/meta
25. Bhaha, P.; Schwarz, K.; Sorantin, P.; and Rickey, S.B.; *Comput. Phys. Commun.*, **1990**, 59, 399. **DOI**: 10. 1016/0010-4655(90)90187-6Z
26. Wu, Z.; Cohen, R. E.; *Phys. Rev. B*, **2006**, 73, 235116. **DOI**:10.1103/PhysRevB.73.235116
27. Blanco, M. A. ; Pendas, A. M. ; Francisco, E. ; Recio, J. M. ;and Franco, R.; *J. Mol. Struct. Theochem.* **1996,** 368, 245-255. **DOI** : 10.1016/S0166-1280(96)90571-0
28. Flo´rez, M.; Recio, J. M.; Francisco, E.; Blanco, M. A.; and Penda´s, A. M.; *Phys. Rev. B*, **2002**, 66. 144112. **DOI:** 10.1103/PhysRevB.66.144112
29. E. Fransisco, J. M. Recio, M. A. Blanco, A. M. Penda´s, and A. Costales, *J. Phys. Chem.*, **1998,** 102, 1595. **DOI**: 10.1021/jp972516j
30. F.D. Murnaghan, *Proc. Natl. Acad. Sci. USA*, **1944**, 30, 244.
31. Yasemin et al. *GU J Sci*, **2014**, 27(2), 761-769.
32. M. Born, K. Huang, Dynamical Theory of Crystal Lattices, Clarendon, 1956.
33. Johnson, R.A.; *Phys. Rev. B*, **1988**, 37, 3924. **DOI**: 10.1103/PhysRevB.37.3924
34. Pettiför, D.G.; *Mater. Sci. Technol.*, **1992**, 8, 345. **DOI**: 10.1179/mst.1992.8.4.345
35. Bannikov, V.V.; Shein, I.R.; Ivanovskii, A.L.*; Phys. Status Solidi RRL*, **2007,** 1, 89. **DOI:** 10.1002/pssr.200600116
36. Pugh, S.F.; *Phil. Mag.*, **1954,** 45, 823. **DOI:** 10.1080/14786440808520496
37. Johnston, G. Keeler, R. Rollins, S. Spicklemire, Solid State Physics Simulations, The Consortium for Upper-Level Physics Software, John Wiley, New York, 1996.

